Available online at www.sciencedirect.com
ScienceDirect
Journal of Photochemistry and Photobiology A: Chemistry 194 (2008) 261–267
Journal of Photochemistry and Photobiology A:Chemistry
www.elsevier.com/locate/jphotochem

Ab initio investigation on the chemical origin of the firefly bioluminescence

Ya-Jun Liu [a,b,*], Luca De Vico [b,**], Roland Lindh [c]

[a] *College of Chemistry, Beijing Normal University, Beijing 100875, PR China*
[b] *Department of Theoretical Chemistry, Chemical Centre, Lund University, P.O. Box 188, S-221 00 Lund, Sweden*
[c] *Department of Chemical Physics, Chemical Centre, Lund University, P.O. Box 188, S-221 00 Lund, Sweden*

Received 14 June 2007; received in revised form 2 August 2007; accepted 21 August 2007
Available online 25 August 2007

Abstract

The chemical origin of the firefly bioluminescence has been investigated by means of density functional and multireference theoretical methods. Different hypotheses on the mechanism of multicolour emission have been investigated: twisting around the central carbon–carbon bond, polarizability of the oxyluciferin microenvironment and presence of resonance structures. The calculated results indicated that the higher the polarizability of the microenvironment is, the larger the red shift of the bioluminescence is. Moreover, a quite flat potential energy surface should allow the easy shifting of the anion minimum between different pseudo-resonance structures. The possible effects of a tight or loose protein pocket has also been considered.

Keywords: Firefly bioluminescence; Chemical origin; DFT; Multireference calculation

1. Introduction

Many different organisms in nature, including bacteria, fungi, fireflies and fishes, are endowed with the ability to emit light. The phenomenon of emitting light as a result of a chemical reaction is called chemiluminescence [1]; when this happens in a living organism it takes the name of bioluminescence [2,3]. Bioluminescence arises from the oxidation of an organic substrate called luciferin (LH2), catalyzed by an enzyme called luciferase [4–6]. Different animals produce very different luciferins, and the specific bioluminescences are also different. However, one common feature to all luciferins is that they must react with molecular oxygen, in order to produce light. Luciferases are oxygenases that utilize molecular oxygen to oxidize luciferins. This oxidation reaction creates a molecule in an electronically excited state. When the molecule returns to a lower electronic energy level it returns the energy in the form of a photon of visible light [7]. The firefly is among the most popular animals showing bioluminescence, and has one of the most efficient bioluminescent systems. In fact, the quantum yield of the bioluminescence reaction is 0.88 [8]. The bioluminescence process could be outlined as Scheme 1.

Two aspects of this process have not been clearly explained yet. One is the chemical mechanism which transforms LH2 into oxyluciferin (OxyLH2), although the analogue small molecule dioxetane has been studied extensively [9–11]. Another one is the chemical origin of the multicolour bioluminescence. This work will focus on the second problem. Fireflies naturally emit yellow-green light (540–580 nm). Interestingly, click beetles and railroad worms use the same luciferin substrate to naturally display light from green to orange and from green to red, respectively [6,7]. In order to explain the variation in the colour of the bioluminescence, five hypotheses have been proposed to date.

(i) White et al. [12] proposed that the excited state of the keto-form of the OxyLH2 anion can relax by emitting red light, while the excited state of the enol-form of the OxyLH2 anion emits yellow-green light. The resulting colour would, then, depend on the keto-enol equilibrium, as Scheme 2 shows. However, the experiments published by Branchini et al. in

* Corresponding author at: College of Chemistry, Beijing Normal University, Beijing 100875, PR China. Tel.: +86 10 5880 1160; fax: +86 10 5880 1160.
** Corresponding author. Tel.: +46 46 222 4500; fax: +46 46 222 4543.
E-mail addresses: yajun.liu@bnu.edu.cn (Y.-J. Liu), luca.de_vico@teokem.lu.se (L. De Vico).

1010-6030/$ – see front matter © 2007 Elsevier B.V. All rights reserved.
doi:10.1016/j.jphotochem.2007.08.022

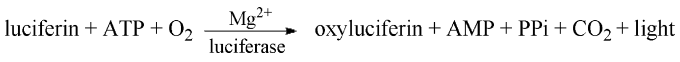

Scheme 1.

2002 [13] demonstrated that the multicolour luminescence requires only the keto-form OxyLH2. Additionally, spectral shifts without changes in the shape have been observed for firefly luciferase mutants [14], which could not be explained by the mechanism proposed by White et al.

(ii) McCapra et al. [15] suggested another mechanism, on the basis of semiempirical theoretical calculations. According to their postulation, the keto-form OxyLH2 in the first singlet excited state (S_1) has a twisted structure rather than a planar one. The planar species is regarded as a saddle point on the S_1 potential energy surface. The colour of the light emission should depend on the rotation around the C–C bond of the –N=C–C=N– moiety. This sounds confusing, since the environment around the C–C bond is strongly conjugative and this bond should have a certain amount of double bond character on the S_1 potential energy surface. The rotation around this C–C bond has to override a large barrier. Brovko et al. [16] and Orlova et al. [17] have confirmed that the planar keto-form and enol-form OxyLH2 are minima on the S_1 potential energy surface, by means of semiempirical and configuration interaction singles (CIS) calculations, respectively. It seems that a mechanism involving 'twisted' conformation to explain colour changes in the firefly bioluminescence is non-feasible.

(iii) The third hypothesis assumes that the colour of the bioluminescence depends on the polarization of the OxyLH2 in the microenvironment of the enzyme–OxyLH2 complex: the higher the polarizability, the larger should be the red shift of bioluminescence [15,18–20]. Time-dependent density functional theory (TD-DFT) calculations apparently support this hypothesis [17]. According to the computed data, the various enol-form of the OxyLH2 anions, enol-s-*trans*(−1), enol-s-*trans*(−2), and enol-s-*trans*(−1)′ (see Figs. 7 and 8 in Ref. [17]), are responsible for the emitted light change from green to red, which is the beetles naturally displayed light [7,21]. Whereas, the keto-s-*trans*, keto-s-*cis*(−1), and keto-s-*trans*(−1) forms of OxyLH2 (see Fig. 10 in Ref. [17] and the corresponding structures in Chart 1 in Ref. [17]) emit light from violet to blue. This does not agree with the experimental conclusion that the multicolour luminescence can be obtained only from the keto-forms [13]. Ref. [17] finally concluded that the participation of the enol-forms of OxyLH2 in bioluminescence is plausible but not required to explain the multicolour emission. Unfortunately, this leaves the chemical origin of the firefly and the other beetles multicolour emission not completely explained.

(iv) Branchini et al. [22] proposed another mechanism in 2004, similar under certain aspects to the first hypothesis. It is suggested that the basis of the mechanism resides in the luciferase modulating the colour emission by controlling the resonance-based anionic keto-form of OxyLH2 excited states. One excited state showing a –N=C–C=N– moiety (keto(−1) in Scheme 3) would relax by emitting green light, another one showing a =N–C=C–N= moiety (keto(−1)′ in Scheme 3) would emit red light.

(v) More recently Nakatsu et al. [23] proposed a control mechanism of the amount of energy loss based on the size of the luciferase protein cavity. In this case, a non-relaxed form of keto OxyLH2 should emit yellow-green light, while after geometrical relaxation it should emit red light. The geometrical relaxation is controlled by the size of the cavity of luciferase, which has been site-specific modified. It remains to be demonstrated if the different cavity allows more freedom to the luciferin substrate, or constraints it in a different structure.

In 2005, Wada and Sakai [24] calculated the decomposition reaction of dioxetanone by semiempirical molecular orbital method, and Goddard's group computed the absorption and emission spectra in both gas phase and aqueous solution [25] by TD-DFT and CIS methods. Quite recently the same group studied the S_1 states of the anionic keto and enol forms of OxyLH2 by multireference calculations [26], and concluded once again that the involvement of the twisted keto or enol forms of anionic OxyLH2 in the bioluminescence is unreasonable. Another rather new paper [27] reported the theoretical study on the colour-tuning mechanism of firefly using symmetry-adapted cluster-configuration interaction (SAC-CI) method in gas phase and protein environment. These recent theoretical studies and experimental observation [18] on the structural

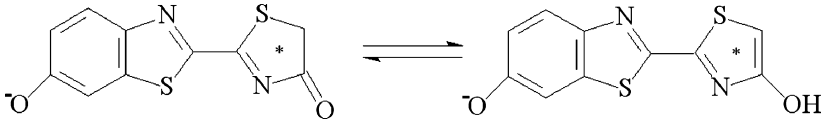

Scheme 2.

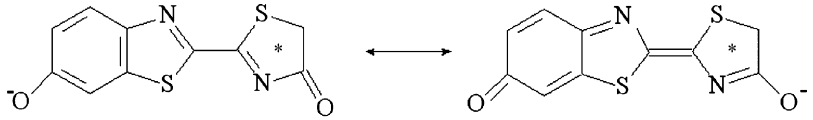

Scheme 3.

basis for the multicolour light of the firefly bioluminescence inspired us to further investigate the chemical origin for the multicolour bioluminescence. In particular it will focus on the following:

- Excluding hypothesis (ii) by employing a higher level of theory method than previous to test the planar nature of keto-form OxyLH2.
- How the polarization of the microenvironment affects the emission of the multicolour light?
- Is the above fourth hypothesis reasonable? If so, are there only two resonance stabilized structures of the excited states of keto-form OxyLH2 anions or more?
- Is the keto-form of OxyLH2 sufficient to fully explain the multicolour emission of the fireflies as suggested by the experiments [13] and [23]?
- Do different protein cavities give more freedom to the substrate, or constrain it in a different structure?

2. Computational methods

This work mainly refers to the calculated properties of four species: the *trans* keto-form of OxyLH2, its two complexes with CH_2Cl_2 and H_2O, and its anion (for convenience, hereafter they are simply referred to as keto-*trans*, keto-*trans* + CH_2Cl_2, keto-*trans* + H_2O, and keto-*trans*(−1), respectively). The DFT method [28], in conjunction with a B3LYP hybrid functional [29,30], was used to optimize their ground state (S_0) geometries and analyze the frequencies. TD [31] DFT-B3LYP method was used to calculate their vertical excitation energies (T_v) and oscillator strengths (*f*). The 6-31+G(d,p) basis set [32] was used for all the atoms. A larger basis set 6-311++G(d,p) was also used for the optimization and frequency calculation of keto-*trans*(−1). Those calculations were performed with the Gaussian 98 program suite [33].

The complete active space SCF (CASSCF) [34] method was used to optimize the S_0 and S_1 geometries of keto-*trans* and several keto-*trans*(−1) resonance structures. Their T_v values and emission (S_1–S_0) transition energies (T_e) were calculated using the multi-state CASPT2 (MS-CASPT2) method [35]. The CASSCF active spaces included most of the lone-pair orbitals of N, O, and S atoms and π orbitals of the systems. Geometry optimizations were carried out using a '14 electrons in 11 orbitals' active space (14-in-11). Later (16-in-14) and (18-in-15) active spaces were used to refine the so found structures. Whereas, for all the T_v and T_e calculations, the selected active spaces were (16-in-14) or (18-in-15). The [He] cores of C, N, and O, and [Ne] core of S were not correlated at the MS-CASPT2 level. The relativistic basis sets of the atomic natural orbital type, ANO-RCC [36], were used for all these multireference calculations. The H basis was contracted to 2s 1p, C, N, O bases were contracted to 3s 2p 1d, and S and Cl to 4s 3p 1d. The scalar relativistic effects were included by the second order Douglas–Kroll–Hess (DKH2) type of transformation [37]. The IPEA modification of the zeroth order Hamiltonian was used [38]. For some structures, the use of an imaginary shift of 0.1 was necessary, in order to remove some intruder state problems [39]. All these calculations were performed using the MOLCAS 6.2 quantum chemistry software [40].

3. Results and discussion

First we will elucidate the restrictions on our choice of structures to be investigated for the purposes of this study. Second, the possible effects of the microenvironment onto the geometry and the emission energies of OxyLH2 will be discussed. Later, we will discuss the possible resonance structures of keto-form OxyLH2 anion, as the fourth hypothesis [22] proposed. In the end, some considerations will be given over the possible spectrum of wavelengths spanned by keto-*trans*(−1) relaxing from the S_1 state, in accordance with hypothesis (v) [23].

3.1. Choice of the structures to study

The experiments [13] suggested that the keto-forms of OxyLH2 are sufficient to obtain multicolour luminescence. Therefore, to confirm this experimental conclusion by theoretical calculation, enol-forms were not considered.

Orlova et al. [17] optimized the geometries of all kinds of keto- and enol-forms of OxyLH2 (for their structures see Chart 1 of Ref. [17]) by B3LYP/6-31+G(d), and concluded that the *trans* conformations of keto, keto(−1), enol, enol(−1), enol(−1)′, and enol(−2) were essentially planar, and that their rigorously planar structures were predicted to be first-order saddle points [17]. The present B3LYP/6-31+G(d,p) calculations, at nearly the same level as Ref. [17] used, predicted that the above mentioned *trans* species are 6.2, 5.4, 6.0, 5.2, 6.2, and 4.9 kcal/mol more stable in energy than their corresponding *cis* conformations, respectively. The frequency analysis of the fully optimized structures indicated that the *trans* conformations of keto, enol, enol(−1), enol(−1)′, and enol(−2) are planar, and have no imaginary frequencies. The fully optimized keto-*trans*(−1) structure shows a dihedral angle S–C–C–S of −179.976°, with one small imaginary frequency, $-46\,cm^{-1}$. However, this small imaginary frequency disappeared when the larger basis set 6-311++G(d,p) was used. So, the keto-*trans*(−1) is also planar. We suppose that the very small imaginary frequencies reported in Ref. [17] could be an artefact of the method, or numerical errors of the calculations. Therefore, we decided to focus our attention only on planar *trans* species, to simplify the field of investigation.

Another purpose of the present study is to understand how the colour of bioluminescence depends on the polarization of OxyLH2 in the microenvironment of the enzyme–OxyLH2 complex. So, we need a series of solvents with different polarizability. Ref. [14] detected the fluorescence spectra of firefly luciferin in eight solvents with different polarizability. For keto-form OxyLH2, Orlova et al. [17] built a simple but reasonable model for the practically complicated environment around it by only considering the polarization of the phenolic OH group of keto. On the basis of this model, we built the simple complexes keto-*trans* + H_2O and keto-*trans* + CH_2Cl_2 by connecting a molecule of H_2O or CH_2Cl_2, the relative small molecules among the eight solvents of Ref. [14], to the phenolic OH

group of keto-*trans*. The orientation polarizability of CH_2Cl_2 and of H_2O are about 0.32 and 0.40, respectively [14]. Obviously, one can consider pure keto-*trans* as in a microenvironment with smallest polarizability, and keto-*trans*(−1) as keto-*trans* in a microenvironment with largest polarizability. We will verify whether keto-*trans*, keto-*trans* + CH_2Cl_2, keto-*trans* + H_2O, and keto-*trans*(−1), representing a gradually increasing polarization of the simulated microenvironment, emit light of gradually increasing wavelengths, as the third hypothesis proposed.

Since one of the purposes of the study is to get some insight on the possible effects of a tight or loose cavity onto the emission colour, the absorption spectra (T_v) or emission ones (T_e) were considered, depending on the case.

3.2. The polarization effect of the microenvironment on keto-trans

In this section we will analyze the possible effects of a tight or loose cavity on keto-*trans*. Different rigid cavities' effects will be simulated as effects coming from microenvironment of different polarizability. The changes induced by a loose cavity will be simulated by relaxing keto-*trans* on the S_1 surface.

The present B3LYP/6-31+G(d,p) optimized minima of keto-*trans* + H_2O and keto-*trans* + CH_2Cl_2 are planar, as the parent molecule. The B3LP/6-31+G(d,p) optimized S_0 geometries of keto-*trans* + CH_2Cl_2 and keto-*trans* + H_2O are depicted in Fig. 1. Certainly, the present DFT optimized bond lengths of keto-*trans* and keto-*trans*(−1) are nearly the same as Ref. [17] reported, since nearly the same method was employed. As can be seen in Fig. 1 and Fig. 5 of Ref. [13], the –N_1–C_1–C_2–N_2– moiety has similar geometry in keto-*trans*, keto-*trans* + CH_2Cl_2, and keto-*trans* + H_2O system, while keto-*trans*(−1) shows about 0.04 Å shorter C_1–C_2 bond, but about 0.03 and 0.02 Å longer N_1–C_1 and C_2–N_2 bonds, respectively.

The T_v and f values of the first three excited states of keto-*trans*, keto-*trans* + CH_2Cl_2, keto-*trans* + H_2O, and keto-*trans*(−1) were calculated at TD-B3LYP/6-31+G(d,p)//B3LYP/6-31+G(d,p) level, and are listed in Table 1. According to Table 1, their first three excited states are $2^1A'$, $1^1A''$, and $3^1A'$ states. The excitation to the second excited state is forbidden, whereas, the S_1 state is electronic dipole allowed and corresponds to a HOMO to LUMO transition. The TD-B3LYP/6-31+G(d,p) calculated T_v values of keto-*trans*, keto-*trans* + CH_2Cl_2, keto-*trans* + H_2O, and keto-*trans*(−1) decrease as the polarization of the microenvironment increases, such that they will emit light of gradually increasing wavelengths, as the hypothesis (iii) proposed. In the framework of a rigid cavity hypothesis, it is possible to affirm that different microenvironment polarizability could affect the emission wavelength.

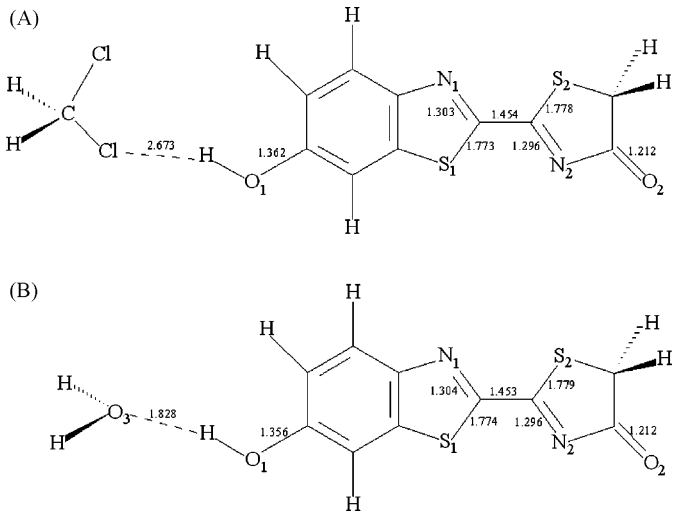

Fig. 1. Selected geometrical parameter (in Å) of (A) keto-*trans* + CH_2Cl_2 and (B) keto-*trans* + H_2O by the B3LYP/6-31+G(d) optimizations.

To explore the possible effects induced by a loose cavity, the S_0 and S_1 geometries of keto-*trans* were optimized by the CASSCF method with the (16-in-14) active space. For the main geometrical parameters see Fig. 2. The MS-CASPT2//CASSCF calculated T_v and T_e values of keto-*trans* are 3.43 and 3.21 eV, respectively. The MS-CASPT2 calculated T_v is 0.11 eV higher than the TD-B3LYP calculated value. The keto-*trans* S_1 is a typical charge-transfer state. Usually, for the charge-transfer states of unsaturated organic molecules, the TD-DFT calculated excitation energies show large errors [41].

It is possible to predict an overall change of ca. 0.2 eV (ca. 40 nm) for the S_1–S_0 energy difference by letting keto-*trans*

Table 1
The TD-B3LYP/6-31+G(d,p) calculated T_v (in eV) and f values of the first three excited states of keto-*trans*, keto-*trans* + CH_2Cl_2, keto-*trans* + H_2O, and keto-*trans*(−1), compared with the available previous calculated results and experimental observations

State	Keto-*trans*		Keto-*trans* + CH_2Cl_2		Keto-*trans* + H_2O		Keto-*trans*(−1)	
	T_v	f	T_v	f	T_v	f	T_v	f
$1^1A'$	0.00		0.00		0.00		0.00	
$2^1A'$	3.32, 3.14[a], 3.35[b]	0.293	3.27	0.336	3.19	0.360	2.54, 2.72[c], 2.39[a], 3.48[d], 2.99[e], 2.87[f]	0.645
$1^1A''$	3.42	0.000	3.44	0.000	3.46	0.000	2.75	0.000
$3^1A'$	3.64	0.268	3.61	0.260	3.57	0.232	3.45	0.255

[a] ZINDO calculation at the optimized B3LYP/6-31+G(d) geometries [17].
[b] Experimentally observed value in aqueous solution at pH 1 [20].
[c] PPP calculation [44] on the LH2 p-electron framework based on crystallographic data [45].
[d] CIS calculation [17].
[e] Experimentally observed value in aqueous solution at pH l0 [20].
[f] Experimentally observed value [43].

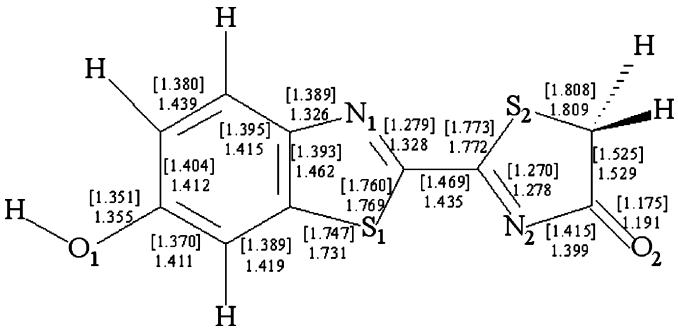

Fig. 2. Selected geometrical parameters (in Å) of S_0 (in square brackets) and S_1 states predicted by the CASSCF/ANO-RCC method for keto-*trans*.

to relax on the excited state before emitting. The MS-CASPT2 calculated T_e value of 3.21 eV is in agreement with the SAC-CI gas phase result of 3.26 eV [27]. However, both of them are outside the range of the visible light, 410 nm (3.02 eV) being the shortest wavelength of visible light [42]. The SAC-CI calculated T_e value of S_1 in dimethyl sulfoxide is found to be 2.95 eV, which is 0.31 eV lower than it in gas phase [27]. This is still much higher than the beetles naturally display visible light from green (λ_{max} ~530 nm, 2.34 eV) to red (λ_{max} 635 nm, 1.95 eV) [7,21]. Even considering the possible shifting of the emission wavelength caused by the protein cavity, the keto-form OxyLH2 molecule can hardly be the chemical origin of the multicolour bioluminescence. Ref. [27] performed the SAC-CI calculations with CIS optimized geometries for keto-*trans*, keto-*trans*(−1), enol-*trans*(−1) and enol-*trans*(−2) inside luciferase. The study concluded that the enol transformation is energetically unfavourable in the luciferase environment and excluded keto-*trans* from the candidates for the chemiluminescence emitter. Since the 2.54 eV TD-B3LYP computed T_v value of keto-*trans*(−1) is closer to the experimentally observed values, we concentrate now on the anionic species.

3.3. The possible structures of keto-trans(−1)

In this section we analyze how to influence the emission of keto-*trans*(−1). At first, in the framework of a tight protein cavity, we will look for possible different resonance structures of the luciferin substrate that might be stabilized by different cavities. Secondly, we will try to understand what could happen if one let the substrate loose.

We failed to locate the S_0 structure of the keto(−1)′ (see Scheme 3) by using the B3LYP/6-31+G(d,p) method. The CASSCF optimization with (14-in-11) active space located two different minima for keto-*trans*(−1) of similar energies. For convenience, we named them as keto(−1a), and keto(−1c). The corresponding geometries are presented in the supporting information. The keto(−1c) geometry is very similar to the structure one obtained by B3LYP/6-31+G(d,p) optimization.

Besides keto(−1a) and keto(−1c), another keto-*trans*(−1) resonance structures was located by CASSCF optimization with the larger active space (16-in-14). We named it as keto(−1b).

The main geometrical parameters of N_1–C_1–N_2–C_2 moiety and the two terminal C–O groups of the three resonance S_0 minima are compared in Table 2. According to their MS-CASPT2 energy, the keto(−1b) is the most stable one, keto(−1a) and keto(−1c) are 2.90 and 1.62 kcal/mol higher, respectively. Keto(−1a) can be associated with the keto(−1)′ structure of Scheme 3, while keto(−1c) with the keto(−1) of the same scheme. Keto(−1b) represents a situation in the middle.

From Table 2, the calculated T_v value of keto(−1a), 2.72 eV, is in agreement with the two experimentally observed values 2.99 eV [20] and 2.87 eV [43]. According to Table 2, when the C_1–C_2 bond length gradually increases, and correspondingly the N_1–C_1 and N_2–C_2 bond lengths gradually decrease, the T_v values also gradually decrease, spanning ca. 0.24 eV (ca. 45 nm). This energy difference is sufficient to transform a yellow-green emitting luciferase into an orange-red one.

The similarities in energies of the three keto-*trans*(−1) forms prompted us to deepen the analysis of the various keto(−1) forms. Each structure was furthermore optimized by employing the even larger active space (18-in-15), along with tighter thresholds. Every structure collapsed to only one global minimum, keto(−1d). The main geometrical parameters are reported in Table 2. Clearly, the previously found structures were local minima on the 'artefact' PES generated by the employed methods. Increasing the active space smoothed such surfaces, leading to the 'true' global minimum. Still, it has to be stressed that, given the small difference in energy among them, a small change in the microenvironment surrounding OxyLH2 should be able to shift the position of the global minimum, towards a different 'resonance' structure than the one reported here. With this respect,

Table 2
The CASSCF optimized main geometrical parameters (in Å) of keto-*trans*(−1)[a] S_0 and S_1 states

Structure	O_1–C_3	O_2–C_4	N_1–C_1	C_1–C_2	C_2–N_2	T_v	T_e
Keto(−1a)	1.208	1.208	1.354	1.371	1.308	2.72	
Keto(−1b)	1.228	1.203	1.320	1.404	1.293	2.59	
Keto(−1c)	1.236	1.190	1.305	1.428	1.279	2.48	
Keto(−1d)	1.230	1.203	1.316	1.401	1.293	2.55	
Keto(−1)*	1.248	1.212	1.301	1.428	1.311		2.20
Keto(−1)*[b]	1.238	1.208	1.311	1.430	1.306		1.84

For each structure, the MS-CASPT2 computed S_1–S_0 energy difference (T_v or T_e) is also given (in eV). The SAC-CI optimized S_1 geometrical parameters and related T_e value are also listed for comparison. Atoms numbering based on Scheme 4.

[a] The selection of active electrons and spaces is 14-in-11 for keto(−1a) and keto(−1c), 16-in-14 for keto(−1b), and 18-in-15 for keto(−1d) and keto(−1)*.

[b] The SAC-CI/6-31G(d) calculated values [27].

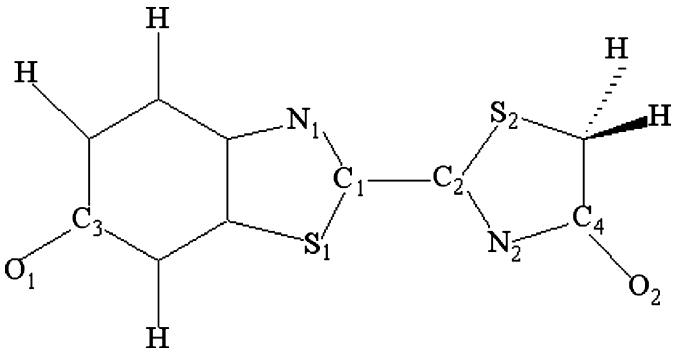

Scheme 4.

hypothesis (iii) and (iv) can be seen as *cause and effect of the same process*. To check this, we performed a geometry scan at fixed C_1–C_2 bond distances (see Scheme 4), while relaxing the rest of the molecule. See supporting information for the so obtained CASSCF profile. The curve is smooth and flat around the minimum, confirming that it should be easy to perturb the structure of the molecule towards a different geometry. The MS-CASPT2 computed energies of some selected points of the curve are presented in Table 3. As can be seen in Table 3, a spanning of ca. 0.15 Å centred on the minimum geometry can be achieved by a perturbation of less than 3 kcal/mol of energy. On the other hand, the energy difference between S_0 and S_1 changes quite much. In fact, in the same range the MS-CASPT2 computed T_v values span ca. 0.2 eV (ca. 40 nm). This means that, following a minimal perturbation from the (micro)environment over the molecule's minimum structure, it is possible to change the wavelength of the emitted radiation. As stated before 40 nm are enough to change a yellow-green emitted light into an orange one.

In order to check how much and in which way the structure of keto-*trans*(−1) can change upon relaxing on S_1, we located one minimum on the S_1 PES, keto(−1)*, by means of the CASSCF method with the larger active space (18-in-15). The main geometrical parameters are reported and compared with the SAC-CI optimized results [27] in Table 2. The MS-CASPT2//CASSCF T_e value is computed to be 2.20 eV, which is to be compared with the SAC-CI//SAC-CI/6-31G(d) result of 1.84 eV—a significant difference which we attribute to the poorer basis set used in the latter investigation. With respect to keto(−1d), allowing the relaxation on S_1 makes keto-*trans*(−1) to "loose" ca. 0.35 eV (ca. 75 nm). Once taken into account a possible shift induced by the protein cavity, it is possible to argue that a loose protein cavity will let the luciferin substrate emit at a very different wavelength than a tight pocket one. Further, the recent SAC-CI study [27] suggested a shift of the emission of −0.01–0.28 eV relative the gas phase value. The two findings resonate well with the suggested control mechanism of Nakatsu et al. [23]. Our ongoing QM(MS-CASPT2)/MM study of oxyLH2 surrounded by different real protein environments will hopefully shed some light on these details.

Table 3
MS-CASPT2 computed relative energies (kcal/mol) and T_v values of selected points along the C_1–C_2 scan (Å)

Structure	C_1–C_2	Relative energy	T_v, eV (nm)
	1.332	2.64	2.66 (466)
Keto(−1d)	1.401	0.00	2.56 (485)
	1.482	2.73	2.45 (506)

4. Conclusions

In order to investigate the mechanism of the chemical origin of the firefly bioluminescence, the *trans* keto-form OxyLH2, its two complexes with CH_2Cl_2 and H_2O, and its anion were studied by means of TD-B3LYP//B3LYP and MS-CASPT2//CASSCF methods. Some conclusions regarding hypothesises (ii)–(v) can be drawn, given that hypothesis (i) has already been taken care of by experimental results. Our results demonstrated that the structure of keto-*trans* and keto-*trans*(−1) are planar, and there is no need for a mechanism involving torsion around C_1–C_2 to explain the multicolour luminescence. The results presented in Section 3.2 showed that it is possible to influence the S_1–S_0 energy difference by different vicinal molecules simulating environments of different polarizability. Even if the model is simple and somehow crude, the difference of polarizability of the microenvironment could be able to reproduce the range of multicolour emission, as stated by hypothesis (iii). Moreover, we showed that, while planar, OxyLH2 is quite flexible. In Section 3.3 we demonstrated how a small amount of energy is required to distort the structure and perturb it such that the S_1–S_0 energy difference changes drastically. This supports hypothesis (iv). As stated before, hypothesis (iii) and (iv) may be seen as cause and effect of the same event. We considered, also, the possible effects resulting from a tight or a loose protein cavity. In particular, we assumed that OxyLH2 in a tight pocket should resemble its S_0 configuration, while in a loose cavity it can relax. We showed how, by relaxing the structure of keto-*trans*(−1) on S_1, it is possible to change dramatically the S_1–S_0 energy difference. This is in line with hypothesis (v).

All our T_v or T_e values were computed as molecules in vacuo, and for this reason they cannot reproduce the natural occurring values of OxyLH2 as embedded in the protein cavity. Anyway, the results are close to the values in solution. What was demonstrated is that a keto-*trans*(−1) structure is capable of emissions at different wavelengths. The mechanisms proposed in hypothesis (iii)–(v) are all plausible. Further more systematic work is still undergoing to elucidate in more details the mechanism of multicolour emission.

Supporting information of the Cartesian coordinates of all the structures discussed in the text and the CASSCF profile scan around S_0 equilibrium geometry is available.

Acknowledgements

This work has been supported by the Swedish Science Research Council (VR) and the Swedish Foundation for Strategic Research (SSF). The LUNARC computer center of Lund University and SNAC are acknowledged for generous allotment of computer resources. LDV acknowledges a grant from the Foundation BLANCEFLOR Boncompagni-Ludovisi née Bildt.

Y.-J. Liu acknowledges funding from the National Natural Science Foundation of China (Grant No. 20673012).

Appendix A. Supplementary data

Supplementary data associated with this article can be found, in the online version, at doi:10.1016/j.jphotochem.2007.08.022.

References

[1] S.E. Braslavsky, K.N. Houk, J.W. Verhoeven, Pure Appl. Chem. 68 (1996) 2223–2286.
[2] W. Adam, G. Cilento, Chemical and Biological Generation of Excited States, Academic Press, New York, 1982.
[3] N.P. Kaplan, N.P. Colowick, M.A. DeLuca, Bioluminescence and Chemiluminescence, Academic Press, New York, 1978.
[4] J.W. Hastings, in: N. Sperelakis (Ed.), Cell Physiology: Source Book, Academic Press, New York, 1995, pp. 665–681.
[5] T. Wilson, Photochem. Photobiol. 62 (1995) 601–606.
[6] K.V. Wood, Photochem. Photobiol. 62 (1995) 662–673.
[7] J.W. Hastings, Gene 173 (1996) 5–11.
[8] H.H. Seliger, W.D. McElroy, Arch. Biochem. Biophys. 88 (1960) 136–141.
[9] Y. Takano, T. Tsunesada, H. Isobe, Y. Yoshioka, K. Yamaguchi, I. Saito, Bull. Chem. Soc. Jpn. 72 (1999) 213–225.
[10] C. Tanaka, J. Tanaka, J. Phys. Chem. A 104 (2000) 2078–2090.
[11] L. De Vico, Y.-J. Liu, J.W. Krogh, R. Lindh, J. Phys. Chem. A 111 (2007) 8013–8019.
[12] E.H. White, E. Rapaport, H.H. Seliger, T.A. Hopkins, Bioorg. Chem. 1 (1971) 92–122.
[13] B.R. Branchini, M.H. Murtiashaw, R.A. Magyar, N.C. Portier, M.C. Ruggiero, J.G. Stroh, J. Am. Chem. Soc. 124 (2002) 2112–2113.
[14] N.N. Ugarova, L.Y. Brovko, Luminescence 17 (2002) 321–330.
[15] F. McCapra, D.J. Gilfoyle, D.W. Young, N.J. Church, P. Spencer, in: A.K. Campbell, L.J. Kricka, P.E. Stanley (Eds.), Bioluminescence and Chemiluminescence: Fundamental and Applied Aspects, John Wiley and Sons, Chichester, 1994, pp. 387–391.
[16] L.Y. Brovko, O.A. Gandelman, W.I. Savich, in: A.K. Campbell, L.J. Kricka, P.E. Stanley (Eds.), Bioluminescence and Chemiluminescence: Fundamental and Applied Aspects, John Wiley and Sons, Chichester, 1994, p. 525.
[17] G. Orlova, J.D. Goddard, L.Y. Brovko, J. Am. Chem. Soc. 125 (2003) 6962–6971.
[18] M. DeLuca, Biochemistry 8 (1969) 160.
[19] N.N. Ugarova, L.Y. Brovko, Russ. Chem. Bull. 50 (2001) 1752–1761.
[20] O.A. Gandelman, L.Y. Brovko, N.N. Ugarova, A.Y. Chikishev, A.P. Shkurimov, J. Photochem. Photobiol. B 19 (1993) 187–191.
[21] W.D. McElroy, H.H. Seliger, in: H. Hayashi, I. Szent-Gyorgyi (Eds.), Molecular Architecture in Cell Physiology, Prentice-Hall, Englewood Cliffs, NJ, 1966, pp. 63–79.
[22] B.R. Branchini, T.L. Southworth, M.H. Murtiashaw, R.A. Magyar, S.A. Gonzalez, M.C. Ruggiero, J.G. Stroh, Biochemistry 43 (2004) 7255–7262.
[23] T. Nakatsu, S. Ichiyama, J. Hiratake, A. Saldanha, N. Kobashi, K. Sakata, H. Kato, Nature 440 (2006) 372–376.
[24] N. Wada, H. Sakai, J. Biol. Phys. 31 (2005) 403–412.
[25] A.-M. Ren, J.D. Goddard, J. Photochem. Photobiol. B: Biol. 81 (2005) 163–170.
[26] T. Yang, J.D. Goddard, J. Phys. Chem. A 111 (2007) 4489–4497.
[27] N. Nakatani, J.-Y. Hasegawa, H. Nakatsuji, J. Am. Chem. Soc. 129 (2007) 8756–8765.
[28] W. Kohn, L.J. Sham, Phys. Rev. 140 (1965) 1133.
[29] C.T. Lee, W.T. Yang, R.G. Parr, Phys. Rev. B 37 (1988) 785–789.
[30] A.D. Becke, J. Chem. Phys. 98 (1993) 5648–5652.
[31] M.E. Casida, C. Jamorski, K.C. Casida, D.R. Salahub, J. Chem. Phys. 108 (1998) 4439–4449.
[32] P.C. Hariharan, J.A. Pople, Theor. Chim. Acta 28 (1973) 213–222.
[33] M.J. Frisch, G.W. Trucks, H.B. Schlegel, G.E. Scuseria, M.A. Robb, J.R. Cheeseman, V.G. Zakrzewski, J.A. Montgomery Jr., R.E. Stratmann, J.C. Burant, S. Dapprich, J.M. Millam, A.D. Daniels, K.N. Kudin, M.C. Strain, O. Farkas, J. Tomasi, V. Barone, M. Cossi, R. Cammi, B. Mennucci, C. Pomelli, C. Adamo, S. Clifford, J. Ochterski, G.A. Petersson, P.Y. Ayala, Q. Cui, K. Morokuma, D.K. Malick, A.D. Rabuck, K. Raghavachari, J.B. Foresman, J. Cioslowski, J.V. Ortiz, A.G. Baboul, B.B. Stefanov, G. Liu, A. Liashenko, P. Piskorz, I. Komaromi, R. Gomperts, R.L. Martin, D.J. Fox, T. Keith, M.A. Al-Laham, C.Y. Peng, A. Nanayakkara, C. Gonzalez, M. Challacombe, P.M.W. Gill, B. Johnson, W. Chen, M.W. Wong, J.L. Andres, C. Gonzalez, M. Head-Gordon, E.S. Replogle, J.A. Pople, Gaussian 98, Gaussian, Inc., Pittsburgh, PA, 1998.
[34] B.O. Roos, P.R. Taylor, Chem. Phys. 48 (1980) 157–173.
[35] B.O. Roos, K. Andersson, M.P. Fülscher, P.-Å. Malmqvist, L. Serrano-Andrés, K. Pierloot, M. Merchán, in: I. Prigogine, S.A. Rice (Eds.), Advances in Chemical Physics, John Wiley & Sons, New York, 1996.
[36] B.O. Roos, R. Lindh, P.-Å. Malmqvist, V. Veryazov, P.-O. Widmark, J. Phys. Chem. A 108 (2004) 2851–2858.
[37] G. Jansen, B.A. Hess, Phys. Rev. A 39 (1989) 6016–6017.
[38] G. Ghigo, B.O. Roos, P.-Å. Malmqvist, Chem. Phys. Lett. 396 (2004) 142–149.
[39] N. Forsberg, P.-Å. Malmqvist, Chem. Phys. Lett. 274 (1997) 196–204.
[40] G. Karlström, R. Lindh, P.-Å. Malmqvist, B.O. Roos, U. Ryde, V. Veryazov, P.-O. Widmark, M. Cossi, B. Schimmelpfennig, P. Neogrady, L. Seijo, Comput. Mater. Sci. 28 (2003) 222–239.
[41] D.J. Tozer, R.D. Amos, N.C. Handy, B.O. Roos, L. Serrano-Andrés, Mol. Phys. 97 (1999) 859–868.
[42] H. Rossotti, Colour, Princeton University Press, 1983.
[43] N. Suzuki, M. Sato, K. Okada, T. Goto, Tetrahedron 28 (1972) 4065.
[44] J. Jung, C.A. Chin, P.S. Song, J. Am. Chem. Soc. 98 (1976) 3949–3954.
[45] D. Dennis, R.H. Stanford, Acta Crystallogr. Sect. B 29 (1973) 1053–1058.